Analytica Chimica Acta 723 (2012) 1–6

Contents lists available at SciVerse ScienceDirect

Analytica Chimica Acta

journal homepage: www.elsevier.com/locate/aca

Dual-color upconversion fluorescence and aptamer-functionalized magnetic nanoparticles-based bioassay for the simultaneous detection of *Salmonella* Typhimurium and *Staphylococcus aureus*

Nuo Duan[a], Shijia Wu[a], Changqing Zhu[b], Xiaoyuan Ma[a], Zhouping Wang[a,*], Ye Yu[b], Yuan Jiang[b]

[a] *State Key Laboratory of Food Science and Technology, School of Food Science and Technology, Jiangnan University, Wuxi 214122, China*
[b] *Jiangsu Entry-Exit Inspection and Quarantine Bureau, Nanjing 210001, China*

ARTICLE INFO

Article history:
Received 17 December 2011
Received in revised form 1 February 2012
Accepted 6 February 2012
Available online 15 February 2012

Keywords:
Aptamer
Salmonella Typhimurium
Staphylococcus aureus
Magnetic nanoparticles
Upconversion nanoparticles

ABSTRACT

A sensitive luminescent bioassay for the simultaneous detection of *Salmonella* Typhimurium and *Staphylococcus aureus* was developed using aptamer-conjugated magnetic nanoparticles (MNPs) for both recognition and concentration elements and using upconversion nanoparticles (UCNPs) as highly sensitive dual-color labels. The bioassay system was fabricated by immobilizing aptamer 1 and aptamer 2 onto the surface of MNPs, which were employed to capture and concentrate *S.* Typhimurium and *S. aureus*. $NaY_{0.78}F_4$:$Yb_{0.2}$,$Tm_{0.02}$ UCNPs modified aptamer 1 and $NaY_{0.28}F_4$:$Yb_{0.70}$,$Er_{0.02}$ UCNPs modified aptamer 2 further were bond onto the captured bacteria surface to form sandwich-type complexes. Under optimal conditions, the correlation between the concentration of *S.* Typhimurium and the luminescent signal was found to be linear within the range of 10^1–10^5 cfu mL^{-1} (R^2 = 0.9964), and the signal was in the range of 10^1–10^5 cfu mL^{-1} (R^2 = 0.9936) for *S. aureus*. The limits of detection of the developed method were found to be 5 and 8 cfu mL^{-1} for *S.* Typhimurium and *S. aureus*, respectively. The ability of the bioassay to detect *S.* Typhimurium and *S. aureus* in real water samples was also investigated, and the results were compared to the experimental results from the plate-counting methods. Improved by the magnetic separation and concentration effect of MNPs, the high sensitivity of UCNPs, and the different emission lines of Yb/Er- and Yb/Tm-doped $NaYF_4$ UCNPs excited by a 980 nm laser, the present method performs with both high sensitivity and selectivity for the two different types of bacteria.

1. Introduction

The rapid and sensitive detection of bacteria count is extremely important in the fields of biotechnology, medical diagnosis, and food safety. In recent years, biosensors have been explored for their application in the detection of pathogenic bacteria [1,2]. The quartz crystal microbalance (QCM) immunosensor is a measurement device initially developed in 1986 for the detection of *Candida albicans* [3]. Thereafter, Xue et al. [4] used CdSe quantum dots to detect the total count of *Escherichia coli* and *Staphylococcus aureus*. The fluorescence method could detect 10^2–10^7 cfu mL^{-1} total count of *E. coli* and *S. aureus* in 1–2 h with a low detection limit of 10^2 cfu mL^{-1}. The use of quantum dots with a single core structure also had limitations, such as the toxicity of heavy metals in their composition, particle growth, photoinduced decomposition, conjugate aggregation, and rapid photobleaching in the presence of oxygen [5]. To overcome these limitations in an effort to develop bioanalytical applications, Fu et al. [6] prepared the core/shell quantum dots (QDs) as a fluorescence probe for bacteria counting, but it had poor sensitivity and could only count bacteria to 3×10^2 cfu mL^{-1}. To improve the detection limit of QCM biosensors, the immunomagnetic particle method was developed for the detection of *E. coli*, and the detection limit was 23 cfu mL^{-1} [7]. However, these immunoassays relied on the specificity of the antigen–antibody reaction, which is not stable.

Aptamers are DNA or RNA molecules that bind to their molecular targets with high affinity and specificity [8–10]. Aptamers have been obtained through in vitro selection or the systematic evolution of ligands by exponential enrichment (SELEX) from a large DNA or RNA library consisting of up to 10^{15} different sequences [11,12]. Aptamers bind to target molecules with similar affinity and specificity as antibodies, yet they possess a variety of advantages over antibodies in both therapeutic and diagnostic applications. For example, aptamers are easy to synthesize, stable, inexpensive, simple to be chemically modified, and minimally immunogenic. Also, aptamers can be modified with a variety of fluorescent dyes or other tags, which provides extraordinary flexibility in the development of assays [13,14]. As a result of this advantage, a number of aptamers have been designed into fluorescent [15], colorimetric

* Corresponding author. Tel.: +86 510 85917023; fax: +86 510 85917023.
E-mail addresses: wangzp@jiangnan.edu.cn, wangzp1974@hotmail.com (Z. Wang).

0003-2670/$ – see front matter © 2012 Elsevier B.V. All rights reserved.
doi:10.1016/j.aca.2012.02.011

[16], and electrochemiluminescence sensors [17] for a wide range of targets.

Lanthanide-doped near-infrared (NIR)-to-visible upconversion nanoparticles (UCNPs) are capable of emitting strong visible fluorescence under the excitation of NIR light (typically 980 nm). UCNPs have shown significant advantages as fluorescent biolabels over the traditional organic fluorophores, due to their attractive optical and chemical features, such as low toxicity, large Stokes shifts, high resistance to photobleaching, blinking, and photochemical degradation. More importantly, excitation of UCNPs biolabels via multi-photon absorption processes allows the use of NIR light, which would not be absorbed by biological samples and induces no autofluorescence and light scattering background [18,19]. As a result, the signal-to-background ratio can be greatly improved. In recent years, with the rapid development of nanostructured materials and nanotechnology in the fields of biotechnology and pathogen detection, magnetic nanoparticles (MNPs) have been receiving considerable attention. Due to their magnetic properties, low toxicity, and biocompatibility, MNPs are useful for the separation of target cells from a mixture of bacteria and matrix substances. Additionally, MNPs help to concentrate the separated cells into a small volume, which is suitable for impedance measurements [20,21].

In this study, we developed a novel and sensitive fluorescence bioassay for the simultaneous detection of *S.* Typhimurium and *S. aureus*. The bioassay system was fabricated by immobilizing aptamer 1 and aptamer 2 onto the surface of MNPs, which were implemented to capture and concentrate *S.* Typhimurium and *S. aureus*, respectively. Due to the high affinity of aptamer to the corresponding bacteria, the aptamer 1-MNPs-*S.* Typhimurium complex subsequently binds to $NaY_{0.78}F_4$:$Yb_{0.2}$, $Tm_{0.02}$ UCNPs modified aptamer 1, and the aptamer 2-MNPs-*S. aureus* bind to $NaY_{0.28}F_4$:$Yb_{0.70}$, $Er_{0.02}$ UCNPs modified aptamer 2. The luminescent signal was effectively amplified with the help of both magnetic separation and concentration. This method demonstrates the first use of aptamer-conjugated magnetic nanoparticles as the capture and concentration element and the use of upconversion nanoparticles as the fluorescence element for the simultaneous detection of two types of pathogenic bacteria.

2. Experimental

2.1. Materials

Rare-earth oxides used in this work, including yttrium oxide (Y_2O_3), ytterbium oxide (Yb_2O_3), erbium oxide (Er_2O_3), and thulium oxide (Tm_2O_3), were of 99.99% purity. Iron trichloride ($FeCl_3{\cdot}6H_2O$), 25% glutaraldehyde ($OHC(CH_2)_3CHO$), and tetraethyl orthosilicate (TEOS) were of analytical grade. All the chemicals above were purchased from Sinopharm Chemical Reagent Co. Ltd. (Shanghai, China). Additionally, 3-Aminopropyltrimethoxysilane (APTES) of 98% purity was purchased from Alfa Aesar (USA). *S.* Typhimurium aptamer (reported by Raghavendra Joshi et al. [22]) and *S. aureus* aptamer (reported by Shao et al. [23]) were synthesized by Shanghai Sangon Biological Science & Technology Company (Shanghai, China). The sequence of the *S.* Typhimurium aptamer was 5′-biotin-C6-TAT GGC GGC GTC ACC CGA CGG GGA CTT GAC ATT ATG ACA G-3′ (aptamer 1). The sequence of the *S. aureus* aptamer was 5′-biotin-C6-GCA ATG GTA CGG TAC TTC CTC GGC ACG TTC TCA GTA GCG CTC GCT GGT CAT CCC ACA GCT ACG TCA AAA GTG CAC GCT ACT TTG CTA A-3′ (aptamer 2).

2.2. Apparatus

Transmission electron microscopy (TEM) was performed using a JEOL model 2100HR instrument operating at 200 kV accelerating voltage (TEM, JEOL Ltd., Japan). X-ray diffraction (XRD) measurements were performed using a D8-advance (Bruker AXS Ltd., Germany) with graphite-monochromatized Cu Kα radiation ($\lambda = 0.15406$ nm). Upconversion nanoparticles fluorescence spectra were measured on an F-7000 fluorescence spectrophotometer (Hitachi, Japan), which was attached to an external 980 nm laser (Beijing Hi-Tech Optoelectronic Co., China) instead of an internal excitation source. The maximum power of the laser was 1300 mW. Ultraviolet–visible (UV–vis) absorption spectra were recorded using a Shimadzu UV-2300 UV-vis spectrophotometer (Shimadzu, Japan). The FT-IR spectra of the bionanoparticles were collected using a Nicolet Nexus 470 Fourier transform infrared spectrophotometer (Thermo Electron Co., U.S.A.) using the KBr method. The suspension of nanoparticles was prepared using an ultrasonic bath KJ-300 (Wuxi Kejie Electron Instruments Co. Ltd., China).

2.3. Bacterial strains and culture media

The *Salmonella* Typhimurium (*S.* Typhimurium) ATCC 50761, *Staphylococcus aureus* (*S. aureus*) ATCC 29213, and *Listeria monocytogenes*, *Escherichia coli ATCC 25922*, and *Vibrio parahemolyticus* ATCC 17802, were obtained from the American Type Culture Collection (ATCC). All *S.* Typhimurium and *S. aureus* were grown under aerobic conditions at 37 °C in BBL Brain Heart Infusion media (BD Difco). *E. coli*, *Listeria*, and *Vibrio parahemolyticus* were grown in Luria-Bertani (LB) (BD Difco).

S. Typhimurium and *S. aureus* ATCC 29213 cells were grown overnight in a liquid culture until an OD_{600} of 0.3 was obtained. Cells were pelleted at 1800×*g* and 4 °C and were washed twice in a 1× binding buffer (1× BB) (50 mM Tris–HCl (pH 7.4), 5 mM KCl, 100 mM NaCl, and 1 mM $MgCl_2$) at room temperature. After incubation at 37 °C for 18 h, colonies on plates were counted to determine the number of colony-forming units per milliliter (cfu mL^{-1}).

2.4. Synthesis and surface modification of $NaYF_4$:Yb/Er, $NaYF_4$:Yb/Tm upconversion nanoparticles (UCNPs)

$NaYF_4$:Yb, Er/Tm UCNPs were synthesized according to method described in our previous work [24,25]. Surface modification of $NaYF_4$:Yb, Er/Tm UCNPs was completed using a typical Stöber-based method [26]. The details of this preparation are shown in the Supplement section.

2.5. Preparation of amine-functionalized Fe_3O_4 magnetic nanoparticles

Amine-functionalized Fe_3O_4 MNPs were prepared according to the method described in Wang's report [27]. This procedure is illustrated in the Supplementary section.

2.6. Preparation of avidin-coated upconversion nanoparticles (UCNPs) and magnetic nanoparticles (MNPs)

A classical glutaraldehyde method [28] was used to conjugate the avidin with the amino groups on the surface of the $NaYF_4$:Yb, Er/Tm UCNPs and MNPs. First, to synthesize the glutaraldehyde-activated composite nanoparticles, amino-activated $NaYF_4$:Yb, Er/Tm UCNPs and MNPs were treated with 5% glutaraldehyde at room temperature for 2 h. The $NaYF_4$:Yb, Er/Tm UCNPs were separated by centrifugation, and the magnetic nanoparticles were magnetically separated and subsequently washed with a phosphate buffer solution three times. After the activation procedure, the surface was covered with avidin by incubating the

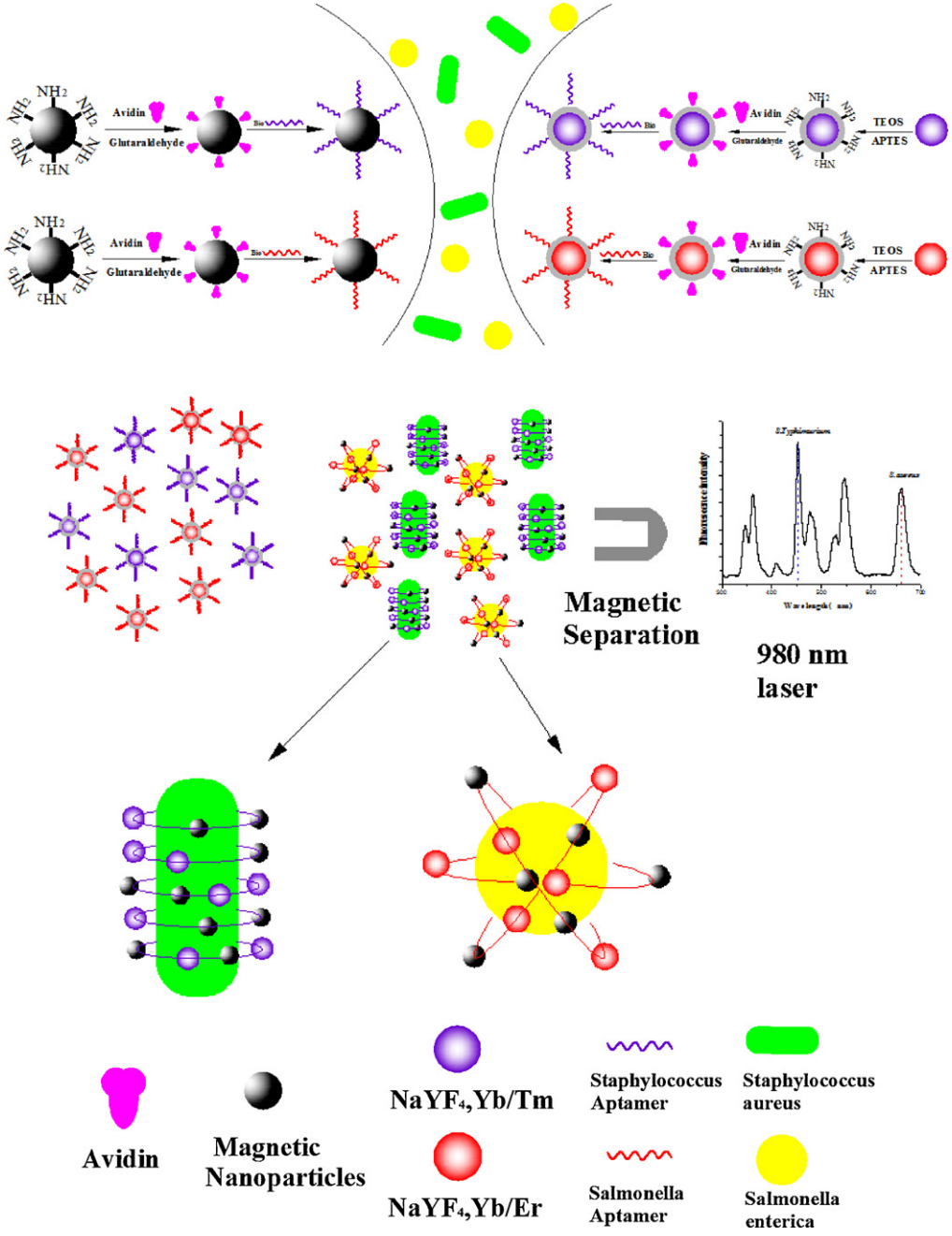

Scheme 1. Fabrication process of biofunctionalized nanoparticles and principle of the performed bioassay. First, aptamer 1 and aptamer 2 were immobilized onto the surface of MNPs and the surface of $NaY_{0.78}F_4$:$Yb_{0.2}$, $Tm_{0.02}$ UCNPs, and $NaY_{0.28}F_4$:$Yb_{0.70}$, $Er_{0.02}$ UCNPs. Next, *S.* Typhimurium and *S. aureus* were added and, due to the highly affinity of aptamer to corresponding bacteria, the aptamer 1-MNPs-*S.* Typhimurium complex bind $NaY_{0.78}F_4$:$Yb_{0.2}$, $Tm_{0.02}$ UCNPs modified aptamer 1, and the aptamer 2-MNPs-*S. aureus* bind $NaY_{0.28}F_4$:$Yb_{0.70}$, $Er_{0.02}$ UCNPs modified aptamer 2. Finally, the luminescent signal was effectively amplified with the help of a magnetic field.

nanoparticles in an avidin solution (125 μg mL^{-1}) overnight to form covalent bonds between the avidin and amino groups.

2.7. Preparation of aptamer-upconversion nanoparticles (UCNPs) conjugates and magnetic nanoparticles (MNPs) conjugates

The aptamer 1 and aptamer 2, which were modified with biotin at their 5′ ends, were used to prepare aptamer-upconversion nanoparticle (UCNP) conjugates and magnetic nanoparticle (MNP) conjugates. Briefly, aptamer 1 (5 μL) was activated with 1 mL of 1 mg mL^{-1} MNPs and $NaYF_4$:Yb, Tm UCNPs. Aptamer 2 (5 μL) was activated with 1 mL of 1 mg mL^{-1} MNPs and $NaYF_4$:Yb, Er UCNPs. After shaking gently for 12 h, oligonucleotides were covalently attached to MNPs and UCNPs through avidin-biotin specific binding followed by blocking the nanoparticles with a 2% bovine serum albumin (BSA) solution. In order to obtain a critical value that can make the surface of MNPs/UCNPs saturated with the aptamers, an indirectly method, based on the final fluorescent intensity, was carried out to determine the optimal concentration of aptamers under the experimental conditions.

2.8. Analytical procedure

Sample solutions containing various concentrations of *S.* Typhimurium and *S.aureus* were prepared in the 1× BB buffer. In a typical test, the sample solution was incubated in 200 μL of

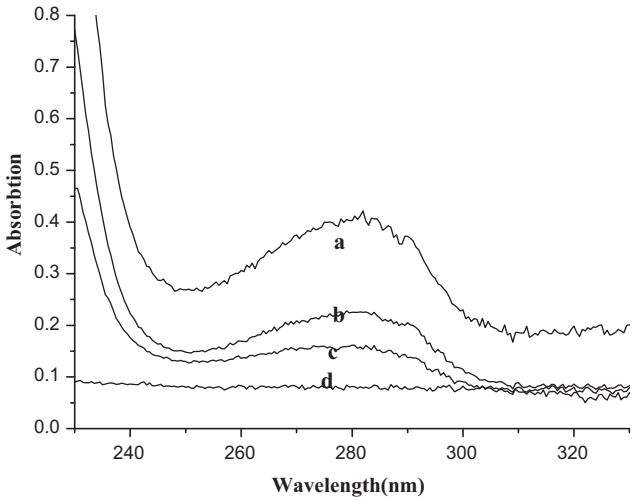

Fig. 1. Absorption spectra of the initial avidin solution (a), supernatant liquor after avidin conjugation to amino-modified $NaYF_4$:Yb, Tm UCNPs (b), supernatant liquor after avidin conjugation to amino-modified $NaYF_4$:Yb, Er UCNPs (c), supernatant liquor after avidin conjugation to amino modified MNPs (d).

aptamer 1-$NaYF_4$:Yb, Tm UCNPs conjugates, 200 μL of aptamer 2-$NaYF_4$:Yb, Er UCNPs conjugates, 80 μL aptamer 1-MNPs conjugates, and 100 μL aptamer 2-MNPs conjugates for 40 min at 37 °C followed by thoroughly washing with the same buffer to remove unbound *S.* Typhimurium and *S. aureus* with an external magnet. Trapped particles were resuspended in 50 μL of PBS and assayed using the F-7000 fluorescence spectrophotometer, which was equipped with a 980 nm laser as the excitation light. This procedure is illustrated in Scheme 1.

3. Results and discussion

Similar to our previous work [26], we prepared $NaYF_4$:Yb/Er, $NaYF_4$:Yb/Tm UCNPs and amine-functionalized Fe_3O_4 MNPs. These nanoparticles were characterized and demonstrated as shown in the Supplementary section.

3.1. Characteristics of avidin-conjugated UCNPs and MNPs

The conjugation of nanoparticles with avidin was characterized using UV–vis spectrophotometry, and the results are shown in Fig. 1. The strong absorbance of avidin before conjugation to nanoparticles can be seen at 210 nm and 280 nm. After incubation of amine-functionalized nanoparticles and avidin, the supernatant was collected by centrifugation and magnetic separation. The absorbance of the supernatant liquor is weaker at 210 nm and 280 nm, which is because part of the avidin combined with amine-functionalized nanoparticles. This result also verified that the nanoparticles were successfully functionalized with amino groups.

3.2. Effect of aptamer concentration

Fig. 2 shows the effect of aptamer concentration on the capture efficiency of the nanoparticles for *S.* Typhimurium and *S. aureus* when the amount of aptamer-MNPs conjugates was fixed at 100 μL. The results show that the capture efficiency increased along with the concentration of the two pathogenic bacteria-specific aptamers immobilized before the bacterial cells were saturated by aptamers on the MNPs. The highest capture efficiency was observed for *S.* Typhimurium and *S. aureus* with 50 nM aptamers. It was observed that the amount of aptamer modified on the MNPs played an important role in the analytical procedure.

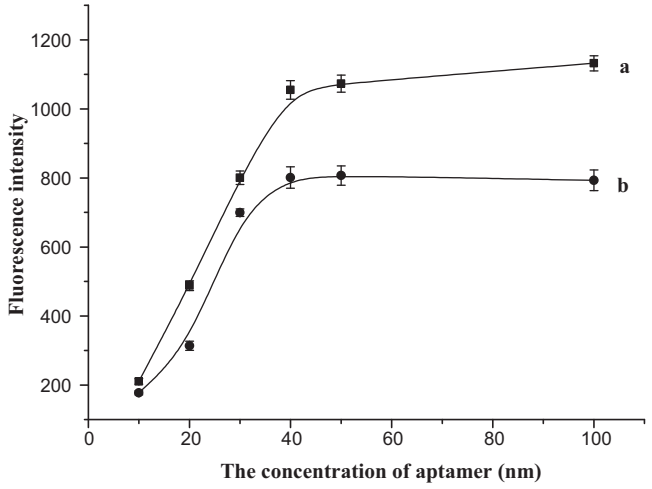

Fig. 2. Fluorescence intensity recorded for signal probes after incubation with various concentrations of aptamers immobilized on MNPs: (a) 200 μL of aptamer 1 functionalized $NaYF_4$,Yb/Tm UCNPs as signal probes for *S.* Typhimurium (10^5 cfu mL^{-1}) and (b) 200 μL of aptamer 2 functionalized $NaYF_4$,Yb/Er UCNPs as signal probes for *S. aureus* (10^5 cfu mL^{-1}), with the fixed volumes of aptamer-MNPs conjugates at 100 μL.

3.3. Effect of the amount of MNPs

It was found that the amount of aptamer-MNPs conjugates greatly influenced the fluorescence intensity of the final MNPs-aptamer/bacteria/aptamer-UCNPs complex. Fig. 3 shows the fluorescence intensity with error bars of *S.* Typhimurium and *S. aureus* for seven samples measured using 20, 40, 60, 80, 100, 120 and 140 μL of aptamer-MNPs conjugates, respectively. It is observed that an increase in the amount of aptamer-MNPs conjugates results in increased fluorescence intensity. We can attribute this observation to the following reasons: MNPs-aptamer 1 and $NaYF_4$:Yb, Tm UCNPs-aptamer 1 have a strong affinity for *S.* Typhimurium, and MNPs-aptamer 2, $NaYF_4$:Yb, Er UCNPs-aptamer 2 have a strong affinity to *S. aureus*. It is expected that the use of increased aptamer-MNPs conjugates leads to a more efficient enrichment of UCNPs and, therefore, a higher fluorescence intensity. However, excess MNPs will deepen the color of the solution

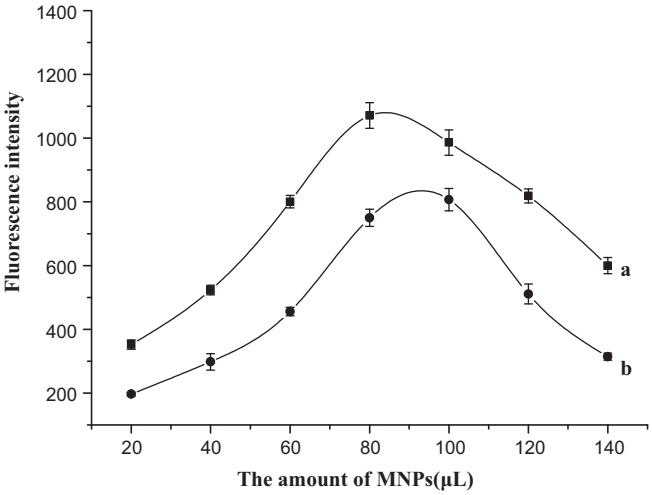

Fig. 3. Fluorescence intensity recorded for signal probes after incubation with various amounts of aptamer-MNPs conjugates: (a) 200 μL of aptamer 1 functionalized $NaYF_4$,Yb/Tm UCNPs as signal probes for *S.* Typhimurium (10^5 cfu mL^{-1}) and (b) 200 μL of aptamer 2 functionalized $NaYF_4$,Yb/Er UCNPs as signal probes for *S. aureus* (10^5 cfu mL^{-1}) with an optimized aptamer concentration of 50 nM.

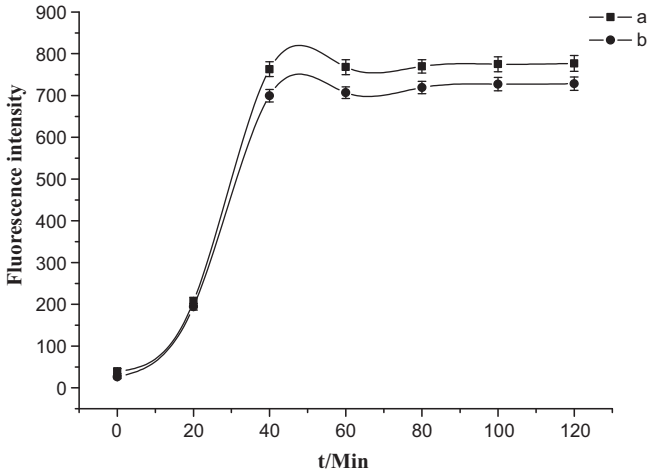

Fig. 4. Fluorescence intensity recorded with various incubation times: (a) 80 μL of aptamer 1 functionalized MNPs and 200 μL of aptamer 1 functionalized $NaYF_4$,Yb/Tm UCNPs as signal probes for *S.* Typhimurium (10^5 cfu mL^{-1}) and (b) 100 μL of aptamer 2 functionalized MNPs and 200 μL of aptamr 2 functionalized $NaYF_4$,Yb/Er UCNPs as signal probes for *S. aureus* (10^5 cfu mL^{-1}).

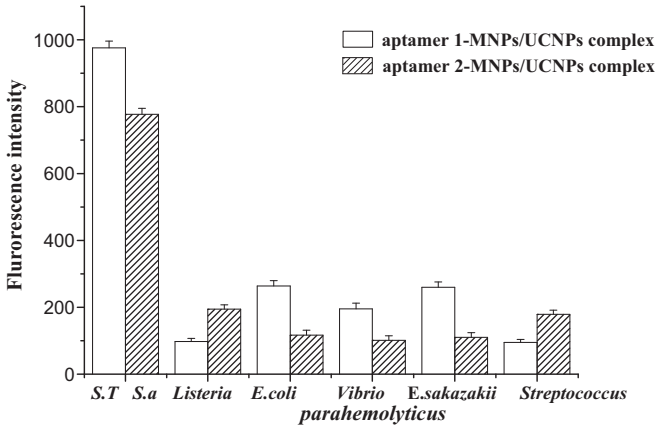

Fig. 5. The intensities measured for *Listeria monocytogenes*, *E. coli*, *Vibrio parahemolyticus*, *E. sakazakii*, *and Streptococcus* in aptamer 1-MNPs, $NaYF_4$,Yb/Tm UCNPs, aptamer 2-MNPs, $NaYF_4$, and Yb/Er UCNPs complexes. The error bars show the standard deviation of three replicate determinations.

(brown into black), thereby leading to decreased fluorescence intensity. Based on these observations, an optimal volume of 80 μL MNPs-aptamer 1 and 100 μL MNPs-aptamer 2 were chosen in the present work.

3.4. Kinetics

To obtain further insight into the kinetics of the fluorescence intensity, we collected the incubation time-dependent fluorescence intensity of the final MNPs-aptamer/bacteria/aptamer-UCNPs complex. Fig. 4 shows the fluorescence intensity of UCNPs as a function of incubation time. In the presence of the target, the curve exhibits a rapid increase in the first 20 min and reaches equilibrium over a period of 40 min, which indicates that the recognition and binding of aptamers to targets is a rapid process. To test the reproducibility of the system, three measurements were obtained under the same conditions.

3.5. Specificity

The specificity of the developed bioassay depends on the aptamers, which can serve as specific ligands for *S.* Typhimurium and *S. aureus*. To investigate the selectivity of the developed bioassay, the fluorescence signal changes that were induced by the binding of five other pathogenic bacteria (*Listeria monocytogenes*, *E. coli*, *Vibrio parahemolyticus*, *E. sakazakii*, *and Streptococcus*) were compared by following the same assay procedure for *S.* Typhimurium and *S. aureus*. Fig. 5 shows that *Listeria monocytogenes*, *E. coli*, *Vibrio parahemolyticus*, *E. sakazakii*, *and Streptococcus* did not exhibit any significant increase in signal. In contrast to the incubation of the aptamer-modified MNPs and UCNPs into the *S.* Typhimurium and *S. aureus*, the signal intensity greatly increased. As a result, the response induced by the non-specific binding was much lower than the response induced by *S.* Typhimurium and *S. aureus*, which shows the high specificity of the bioassay.

3.6. Analytical performance

In a typical experiment, different concentrations of *S.* Typhimurium and *S. aureus* were added to the aptamer conjugated MNPs and UCNPs and incubated for 40 min at 37 °C. Based on the specific affinity of aptamer to bacteria, the upconversion and magnetic nanoparticles biocomplex was formed. This complex was subsequently concentrated and separated using magnetic separation. We chose the emission of 452 nm and 660 nm to monitor *S.* Typhimurium and *S. aureus* because the two emission peaks will not interfere with each other in the fluorescent spectrum of the mixed signal probes. In the absence of pathogenic bacteria, the luminescent intensity was at a minimum, and in the presence of the different concentrations of *S.* Typhimurium and *S. aureus*, the fluorescent signal of the nanocomposite varied. Under optimal conditions, the concentration of bacteria is proportional to the increased luminescent intensity (ΔI) in which ΔI represents the difference of upconversion luminescent intensity excited by the 980 nm laser in the absence and in the presence of *S.* Typhimurium and *S. aureus*. Various intensities of fluorescent spectra obtained in the presence of different concentrations of *S.* Typhimurium and *S. aureus* (log cfu mL^{-1}) are shown in Fig. 6a. A strong linear correlation ($R^2 = 0.9964$) was obtained between 10^1 and 10^5 cfu mL^{-1} *S.* Typhimurium concentration. Accordingly, Fig. 6b shows the linear relationship between the relative intensity of the upconversion luminescence and the concentration of *S. aureus*, the intensity of upconversion luminescence varied linearly with the concentration of *S.aureus* in the solution from 10^1 to 10^5 cfu mL^{-1} ($R^2 = 0.9936$). The sensitivity of the developed immunoasssay was investigated, and the LODs of the proposed method for *S.* Typhimurium and *S. aureus* were found to be 5 cfu mL^{-1} and 8 cfu mL^{-1}, respectively.

3.7. Analytical application

The accuracy of the applied bioanalysis method was evaluated with real water samples, such as lake, stream, and puddle samples. The three real water samples were left to stand for 30 min to precipitate macroaggregate and seston. Then the supernatant was treated with 0.45 μm filtration membrane. And the results obtained were compared to those of the classical counting methods. The analysis

Table 1
Comparison of the results obtained from the analysis of real water samples using the bioassay and classical counting methods.

Water sample	Plate counting method (cfu mL^{-1})		Proposed method (cfu mL^{-1})	
	S. Typhimurium	*S. aureus*	*S.* Typhimurium	*S. aureus*
Lake	31 ± 1.4	26 ± 4.6	21 ± 1.4	27 ± 3.8
Stream	85 ± 4.2	88 ± 2.9	80 ± 3.5	76 ± 2.5
Puddle	228 ± 5.7	235 ± 2.2	218 ± 4.5	222 ± 3.0

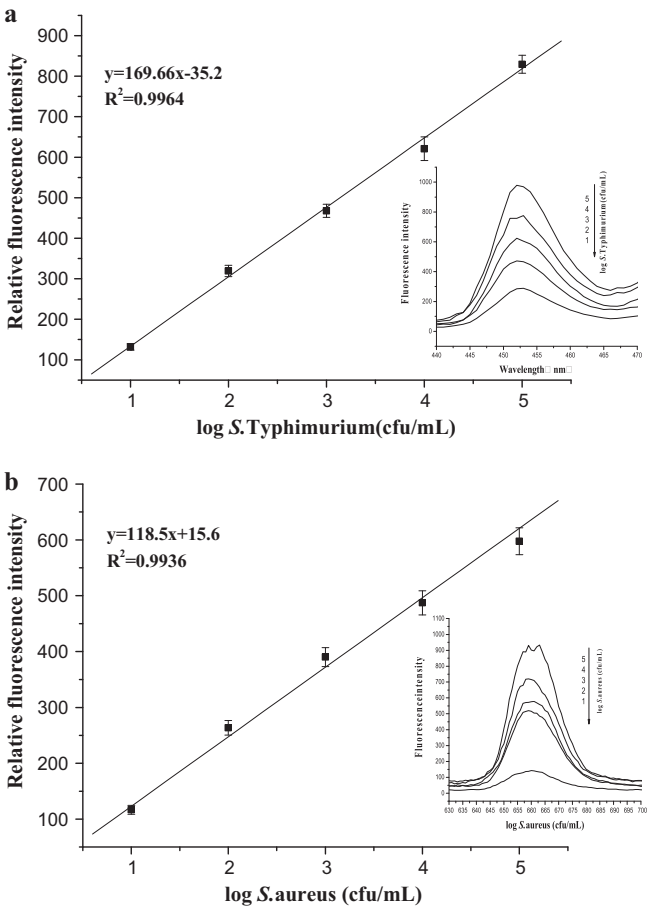

Fig. 6. Standard curve of the increased luminescent intensity (ΔI) versus *S.* Typhimurium concentration measured using the developed method (a), a typical recording output for the detection of different concentrations *S.* Typhimurium using the developed method (inset a), a standard curve of the increased luminescent intensity (ΔI) versus *S. aureus* concentration measured using the developed method (b), and a typical recording output for the detection of different concentrations of *S. aureus* using the developed method (inset b).

results are given in Table 1. The concentration of *S.* Typhimurium and *S. aureus* were determined for the lake, steam, and puddle samples. The results obtained using the developed bioassay were similar to those obtained using the plate counting method. There was no significant difference between the methods that were compared.

4. Conclusion

In this study, an aptasensor based on magnetic nanoparticles coupled with upconversion nanoparticles was successfully developed and evaluated for the simultaneous, rapid, and specific detection of both *S.* Typhimurium and *S. aureus*. The use of aptamer-functionalized magnetic nanoparticles and upconversion nanoparticles probes provided an efficient and specific way to capture and concentrate bacteria with the help of a magnetic field, and the luminescent signal was also effectively amplified. In addition, aptamers are stable at room temperature, unlike traditional antibodies, which are vulnerable to degradation with temperature changes. The detection limits of the bioassay were 5 cfu mL^{-1} for *S.* Typhimurium and 8 cfu mL^{-1} for *S. aureus*. The present biosensing method may be easily adopted for the detection of other bacterial pathogens by substituting suitable aptamers, showing this assay's great potential in food safety control. Any autofluorescence originating from biomolecules possibly contained in solution can also be entirely avoided, due to the use of infrared 980-nm laser excitation. Therefore, this assay offers a new approach to fabricate a convenient, sensitive, and stable platform for nanolabel applications for bioassays.

Acknowledgments

This work was partly supported by National S&T Support Program of China (2012BAK08B01, 2011BAK10B03), the S&T Supporting Project of Jiangsu Province (BE2011621, BE2010679), Mérieux Research Grant Program, and Research Fund for the Doctoral Program of Higher Education (20110093110002), and Program for New Century Excellent Talents in University (NCET-11-0663).

Appendix A. Supplementary data

Supplementary data associated with this article can be found, in the online version, at doi:10.1016/j.aca.2012.02.011.

References

[1] X.L. Su, Y. Li, Biosens. Bioelectron. 21 (2005) 840–848.
[2] M. Varshney, Y. Li, Biosens. Bioelectron. 22 (2007) 2408–2414.
[3] H. Muramatsu, K. Kajiwara, E. Tamiya, I. Karube, Anal. Chim. Acta 188 (1986) 257–261.
[4] X.H. Xue, J. Pan, H.M. Xie, J.H. Wang, S. Zhang, Talanta 77 (2009) 1808–1813.
[5] K.B. Male, B. Lachance, S. Hrapovic, G. Sunahara, J.H.T. Luong, Anal. Chem. 80 (2008) 5487–5493.
[6] X. Fu, K.L. Huang, S.Q. Liu, Anal. Bioanal. Chem. 396 (2010) 1397–1404.
[7] Z.Q. Shen, J.F. Wang, Z.G. Qiu, M. Jin, X.W. Wang, Z.L. Chen, J.W. Li, F.H. Cao, Biosens. Bioelectron. 26 (2011) 3376–3381.
[8] H.S. Mader, P. Kele, S.M. Saleh, O.S. Wolfbeis, Curr. Opin. Chem. Biol. 14 (2010) 582–596.
[9] F. Wang, X. Liu, Chem. Soc. Rev. 38 (2009) 976–989.
[10] M.E. Piyasena, L.J. Real, R.A. Diamond, H.H. Xu, F.A. Gomez, Anal. Bioanal. Chem. 392 (2008) 877–886.
[11] M. Varshney, Y.B. Li, Biosens. Bioelectron. 22 (2007) 2408–2414.
[12] L.C. Bock, L.C. Griffin, J.A. Latham, E.H. Vermaas, J.J. Toole, Nature 355 (1992) 564–566.
[13] A.D. Ellington, J.W. Szostak, Nature 355 (1992) 850–852.
[14] L. Gold, B. Polisky, O. Uhlenbeck, M. Yarus, Annu. Rev. Biochem. 64 (1995) 763–797.
[15] R.R. Breaker, Curr. Opin. Chem. Biol. 1 (1997) 26–31.
[16] C. Tuerk, L. Gold, Science 249 (1990) 505–510.
[17] C.L.A. Hamula, J.W. Guthrie, H. Zhang, X.F. Li, X.C. Le, Trends Anal. Chem. 25 (2006) 681–691.
[18] M. Teresa, C.Ö. Veli, L.S. Pablo, M. Mònica, K. Ioanis, K.O. Ciara, Anal. Bioanal. Chem. 390 (2008) 989–1007.
[19] S. Nagatoishi, T. Nojima, E. Galezowska, A. Gluszynska, B. Juskowiak, S. Takenaka, Anal. Chim. Acta 581 (2007) 125–131.
[20] J. Liu, Y. Lu, Angew. Chem. Int. Ed. 45 (2006) 90–94.
[21] Z.P. Wang, N. Duan, X. Hun, S.J. Wu, Anal. Bioanal. Chem. 398 (2011) 2125–2132.
[22] J. Raghavendra, J. Harish, P.D. Hari, T.M.A. Senthil Kumar, L.A. Jaykus, Mol. Cell. Probes 23 (2009) 20–28.
[23] X.X. Cao, S.H. Li, L.C. Chen, H.M. Ding, H. Xu, Y.P. Huang, J. Li, N.L. Liu, W.H. Cao, Y.J. Zhu, B.F. Shen, N.S. Shao, Nucl. Acids Res. 37 (2009) 4621–4628.
[24] S.J. Wu, N. Duan, Z.P. Wang, H.X. Wang, Analyst 136 (2011) 2306–2314.
[25] S.J. Wu, N. Duan, C.Q. Zhu, X.Y. Ma, M. Wang, Z.P. Wang, Biosens. Bioelectron. 30 (2011) 35–42.
[26] W. Stöber, A. Fink, J. Colloid Interface Sci. 26 (1968) 62–69.
[27] L.Y. Wang, L. Wang, F. Zhang, Y.D. Li, Chem. Eur. J. 12 (2006) 6341–6347.
[28] Z.Q. Ye, M.Q. Tan, G. Wang, J.L. Yuan, Anal. Chem. 76 (2004) 513–518.